GEOPHYSICAL RESEARCH LETTERS, VOL. 34, L19807, doi:10.1029/2007GL030752, 2007

A missing sink for gas-phase glyoxal in Mexico City: Formation of secondary organic aerosol

Rainer Volkamer,[1,2] Federico San Martini,[3] Luisa T. Molina,[4,5] Dara Salcedo,[6] Jose L. Jimenez,[2] and Mario J. Molina[1]

Received 21 May 2007; revised 23 July 2007; accepted 17 August 2007; published 9 October 2007.

[1] The sources of secondary organic aerosol (SOA) are highly uncertain. Direct measurements of gas-phase glyoxal in Mexico City are compared to experimentally constrained model predictions. Observed glyoxal concentrations are found significantly below those predicted. Additional glyoxal sources are likely and would increase these differences; an additional glyoxal sink must be operative. The model-measurement differences are fully resolved by a sink parameterized from aerosol parameters as either (1) irreversible uptake to aerosol surface area (uptake coefficient $\gamma \approx 0.0037$); reversible partitioning to (2) aerosol liquid water (effective Henry's law coefficient $H_{eff} \approx 4 \times 10^9$ M atm^{-1}), or (3) the oxygenated organic aerosol phase (activity coefficient $\zeta \approx 6 \times 10^{-9}$); (4) a combination of the above. The missing sink has the potential to determine 70–95% of the atmospheric lifetime of glyoxal. The glyoxal imbalance corresponds to several μg m^{-3} of equivalent SOA mass, and can explain at least 15% of the SOA formation in Mexico City. **Citation:** Volkamer, R., F. San Martini, L. T. Molina, D. Salcedo, J. L. Jimenez, and M. J. Molina (2007), A missing sink for gas-phase glyoxal in Mexico City: Formation of secondary organic aerosol, *Geophys. Res. Lett.*, *34*, L19807, doi:10.1029/2007GL030752.

1. Introduction

[2] In urban air, first-generation oxidation products from anthropogenic volatile organic compounds (VOCs) contribute significantly to SOA formation. The timescale and amounts of SOA production are currently not captured by photochemical models [*Volkamer et al.*, 2006]. Glyoxal (CHOCHO), the smallest α-dicarbonyl, forms as a first generation oxidation product from numerous VOCs [*Calvert et al.*, 2000; *Volkamer et al.*, 2001]. Despite its high volatility – the vapor pressure of glyoxal [*Kielhorn et al.*, 2004] is about 6 orders of magnitude too high to explain physical partitioning to the aerosol organic phase – a growing body of laboratory studies report evidence for uptake to particles [*Jang et al.*, 2002; *Liggio et al.*, 2005a; *Kroll et al.*, 2005] and cloud droplets [*Schweitzer et al.*, 1998; *Lim et al.*, 2005; *Loeffler et al.*, 2006] due to chemical reactions that lead to the formation of low-volatility products. For particles, the atmospheric relevance and mechanism of this sink for gas-phase glyoxal are presently not clear. Depending on whether a reversible or irreversible mechanism is assumed, glyoxal uptake accounts either for several 10 ng m^{-3} or several 10 μg m^{-3} of equivalent SOA mass in urban air [*Kroll et al.*, 2005; *Liggio et al.*, 2005a]. Further, conflicting evidence exists about the role of acid-catalysis in controlling the reactive uptake of glyoxal on particles [*Jang et al.*, 2002; *Liggio et al.*, 2005a; *Kroll et al.*, 2005].

[3] Glyoxal is a novel indicator molecule for active VOC photochemistry on global scales. The direct spectroscopic detection of glyoxal in the atmosphere indicated the feasibility of measuring glyoxal by solar-straylight techniques [*Volkamer et al.*, 2005a], which has since been demonstrated from space-borne platforms [*Kurosu et al.*, 2005; *Wittrock et al.*, 2006] and from the ground [*Sinreich et al.*, 2007]. In order to accurately represent glyoxal in models a detailed understanding of sources and sinks is needed.

2. Measurements and Calculations

[4] High time-resolution glyoxal measurements by long-path Differential Optical Absorption Spectroscopy (LP-DOAS) were conducted as part of the Mexico City Metropolitan Area Field Campaign (MCMA-2003) and provide novel means to test predictions by photochemical models [*Volkamer et al.*, 2005a]. The budget of gas-phase glyoxal has not been studied directly to date.

[5] In the MCMA the glyoxal source from VOC oxidation (41 VOC precursors are currently identified [*Volkamer et al.*, 2005c]) is much larger than direct vehicle emissions; little is known about emissions from point sources but the lack of sharp plumes suggest that they are minor contributors [*Volkamer et al.*, 2005a]. We have developed a first generation glyoxal model (FGM) that calculates glyoxal production from the oxidation of 26 VOCs as listed in Table 1. VOCs are included in the FGM only if direct measurements of their concentration [*Velasco et al.*, 2007, T. Jobson et al., Intercomparison of volatile organic carbon measurement techniques and data from the MCMA 2003 field experiment, submitted to *Atmospheric Chemistry and Physics Discussion*, 2007, hereinafter referred to as T. Jobson et al., submitted manuscript, 2007] and relevant oxidants (OH-radicals, O_3) [*Shirley et al.*, 2006; *Volkamer et al.*, 2007] are available. Most of the yields listed in Table 1 have been quantified in laboratory studies [*Calvert et al.*,

[1]Department of Chemistry and Biochemistry, University of California, San Diego, La Jolla, California, USA.
[2]Department of Chemistry and Biochemistry and Cooperative Institute for Research in Environmental Sciences, University of Colorado, Boulder, Colorado, USA.
[3]Board on Chemical Sciences and Technology, National Academies, Washington, D. C., USA.
[4]Department of Earth, Atmospheric, and Planetary Science, Massachusetts Institute of Technology, Cambridge, Massachusetts, USA.
[5]MCE2, La Jolla, California, USA.
[6]Centro de Investigaciones Químicas, Universidad Autónoma del Estado de Morelos, Cuernavaca, Mexico.

0094-8276/07/2007GL030752$05.00

Table 1. Production and Loss Rates, Sink Parameters, and Lifetime of Glyoxal for 9 April 2003

Parameter	Yield	11 am	3 pm
MCM prod. rate [ppt hr^{-1}]		615	2005
FGM, %		77.7	72.4
MCM-FGM, %		22.3	27.6
VOC + OH reactions		87.6	78.2
VOC + O_3 reactions		12.4	21.8
Aromatics, %		78.7	69.8
benzene, %	32.0	1.0	1.0
toluene, %	30.6	34.7	41.2
p-xylene, %	31.9	8.7	4.5
m-xylene, %	7.9	11.0	8.3
o-xylene, %	8.0	1.5	1.4
124-TMB, %	7.2	3.8	3.4
123-TMB, %	7.8	0.7	0.7
ethylbenzene, %[a]	30.6	4.7	2.0
propylbenzene, %[a]	30.6	0.9	0.4
iso-propylbenzene, %[a]	30.6	7.8	3.3
p-ethyltoluene, %[a]	31.9	3.0	2.8
m-ethyltoluene, %[a]	7.9	0.6	0.5
o-ethyltoluene, %[a]	8.0	0.3	0.3
Alkenes, %		13.4	22.7
ethene, %	0.44	0.03	0.06
propene, %	8.3	1.0	1.8
1-butene, %	0.3	0.02	0.04
cis-2-butene, %	11.3	1.6	2.9
trans-2-butene, %	14.7	3.7	6.6
2-methyl-2-butene, %	4.5	3.0	5.2
2-methylpropene, %	0.5	0.04	0.07
butadiene, %	0.4	0.003	0.006
1-pentene, %	2.0	0.02	0.04
2-methyl-1-butene, %	0.4	0.02	0.03
2-methyl-2-butene, %	4.5	3.0	5.2
isoprene, %	3.0	1.0	0.9
Acetylene, %	63.5	7.9	7.5
Lifetime, min			
reversible sink		170	127
irreversible sink		49	30
Total loss rate, $\times 10^{-4}$ s^{-1} [b]		3.4	5.5
photolysis, %[b]		4.5	10.3
OH-reaction, %[b]		2.7	5.7
dry deposition, %[b]		0.6	0.4
dilution, %[b]		5.2	6.4
irreversible sink, %		80.8	77.2
MCM_γ, γ, 10^{-3}		$4.2^{+5.9}_{-2.0}$	$2.5^{+2.2}_{-1.2}$
MCM_{Heff}, ρ 10^8		$10^{+4.8}_{-4.6}$	$5.2^{+2.8}_{-2.0}$
MCM_{Peff}, ζ, 10^{-9}		$3.8^{+2.8}_{-1.1}$	$8.4^{+7.9}_{-2.5}$

[a]No experimental yield available, estimated value.
[b]Under the assumption of irreversible glyoxal loss.

2000; *Volkamer et al.*, 2001; *Calvert et al.*, 2002]; for a few species we use estimates of yields that rely on measurements of structurally similar compounds [*Bloss et al.*, 2005; *Volkamer et al.*, 2005b]. FGM calculates only the portion of glyoxal that forms as a first generation oxidation product, ignores other sources, and hence calculates a lower-limit glyoxal production rate. We also use a second model that is based on the Master Chemical Mechanism, MCM (v3.1) [*Bloss et al.*, 2005] constrained for the same 26 VOCs; MCM calculates additional glyoxal that forms as a second and higher generation oxidation product (secondary glyoxal). Active steps had been taken during the development of MCMv3.1 to minimize secondary glyoxal from aromatic VOCs [*Bloss et al.*, 2005] reflecting results from [*Volkamer et al.*, 2001] that indicated that this route is not significant. We have modified our version of MCM, to reflect a re-evaluation of those yields [*Volkamer et al.*, 2005b], which gave slightly lower and more precise yield numbers.

[6] During the day, rapid photolysis and OH-reactions limit the atmospheric lifetime to few hours [*Volkamer et al.*, 2005a]. Glyoxal loss processes in both models include: (1) photolysis (measured by spectroradiometry as described previously [*Volkamer et al.*, 2005a], using more precise photochemical parameters [*Volkamer et al.*, 2005b; *Tadic et al.*, 2006]); (2) reaction with OH-radicals (rate constant $k = 9.2 \times 10^{-12}$ cm^3 $molec^{-1}$ s^{-1} [*Feierabend et al.*, 2006]), both of these gas-phase losses are quantified with good confidence (better than 25%); (3) an upper limit estimate of dry deposition (assuming a dry deposition velocity v = 0.3 cm/s, and negligible resistance at the ground); and (4) dilution in a rising planetary boundary layer (PBL) as described previously [*de Foy et al.*, 2005; *Volkamer et al.*, 2006, 2007]. We have implemented glyoxal losses to aerosols in three ways: the first model termed "MCM_γ" parameterizes an irreversible glyoxal sink as a mono-exponential loss rate $k_{AER} = \gamma \times S \times 8.5\ 10^{-4}$, where γ represents an effective uptake coefficient of glyoxal (fraction of collisions between glyoxal and the surface leading to uptake), S is the condensational sink surface area of fine particulate matter; the constant factor accounts for conversion to units of s^{-1}. The condensational sink surface area was calculated from the mass distributions vs. aerodynamic diameter measured by the aerosol mass spectrometer (AMS), supplemented by including black carbon (with the size distribution of AMS m/z 57) and crustal material (with its measured size distribution by PIXE) as described in [*Salcedo et al.*, 2006], aerosol liquid water (*ALW*, with the inorganic size distribution), and taking into account diffusion limitations on mass transfer rates [*Pirjola et al.*, 1999]. *ALW* was predicted by a Markov Chain Monte Carlo model, integrating observations of aerosol inorganic species and gas-phase ammonia with the thermodynamic equilibrium model ISORROPIA [*San Martini et al.*, 2006]. We use the model to predict particle acidity (*pH*) and ionic strength (*IS*). A second model version "MCM_{Peff}" reversibly partitions glyoxal with an effective vapor pressure $P_{eff} = \zeta \times P_{vap}$ in the oxygenated organic aerosol (*OOA*, measured by the AMS), where ζ is the organic phase activity coefficient [*Pankow*, 1994], and P_{vap} = 223 Torr (at 20 C) is the vapor pressure of glyoxal [*Kielhorn et al.*, 2004]. Analogously, a third model version "MCM_{Heff}" reversibly partitions gas-phase glyoxal into *ALW* according to Henry's Law with an effective constant $H_{eff} = \rho \times H$, where ρ is the aqueous phase activity coefficient, and H = 5 M atm^{-1} is the physical solubility of glyoxal in water [*Schweitzer et al.*, 1998]. Finally, the γ, ζ and ρ parameters were derived by minimizing least-squares to bring predicted gas-phase glyoxal into agreement with observed glyoxal; uncertainties in Table 1 represent the combined (model + measurement) 2σ uncertainty.

[7] We apply these models to our previous SOA case study of 9 April 2003, when about 85% of the observed SOA mass is unaccounted by a model that considers traditional SOA precursor VOCs [*Volkamer et al.*, 2006]. Briefly a "Norte" meteorological event brought clean, cool,

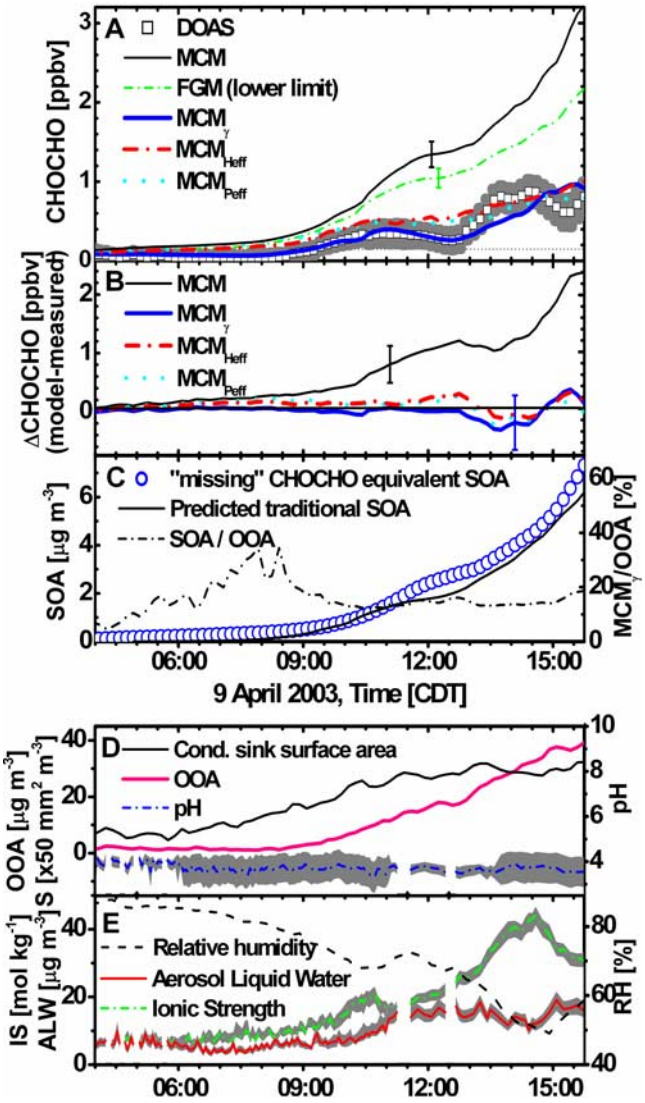

Figure 1. Comparison of gas-phase CHOCHO observations (DOAS, measurement uncertainty shaded in grey) with experimentally constrained predictions. (A) FGM lower-limit glyoxal production (dash-dotted line), MCM (solid thin line), MCM_{γ} (solid thick line), MCM_{Heff} (dashed line), and MCM_{Peff} (dotted line). (B) Model-measurement differences for MCM, MCM_{γ} ($\gamma = 0.0037$), MCM_{Heff} ($\rho = 8 \times 10^8$), and MCM_{Peff} ($\zeta = 6 \times 10^{-9}$). (C) Comparison of the glyoxal imbalance expressed as equivalent SOA mass with OOA observations (dash-dotted line) and SOA modeling (solid line) [*Volkamer et al.*, 2006]. (D, E) Characterization of *ALW*, *S*, *pH*, *IS* (as defined in the text) and relative humidity.

and humid air to the city [*de Foy et al.*, 2005]. The day starts with low pollutant concentrations, followed by rush-hour traffic emissions (starting around 6 am CDT = UTC − 5h) and the onset of the photochemistry around 8 am. Wind speed is low (1–3 m s^{-1}) throughout the day, so that the air arriving at the site has been over the city for several hours. Vertical mixing is reduced compared to other days; dust and biomass burning events are suppressed from preceding periods of rain which is confirmed by the lowest levels of aerosol K of the campaign [*Johnson et al.*, 2006]. For these reasons the case can be treated approximately as a chemical box model with vertical (boundary layer) dilution. Other days were studied using adjusted dilution scenarios, and yielded similar results to those described here.

3. A Missing Sink for Glyoxal

[8] Both models ignore glyoxal sources from unmeasured glyoxal precursor VOCs, car exhaust (estimated a minor source in the MCMA, i.e., 4% [*Volkamer et al.*, 2005a; *Garcia et al.*, 2006]), and calculate glyoxal formation conservatively. Additional sources are likely and would increase predicted glyoxal concentrations. Glyoxal is mostly produced from reactions of aromatic VOC with OH-radicals; the contribution from O_3 + alkene reactions increases in the afternoon (Table 1). About 8% of the glyoxal source is from the acetylene + OH reaction. Secondary glyoxal production can be estimated from the difference between the FGM and MCM models; it accounts for about a quarter of the glyoxal production rate, indicating that the photochemical production is well constrained.

[9] During the night and throughout the day both models consistently predict higher glyoxal concentrations than were observed (Figure 1a). Glyoxal predicted by MCM is 2–6 times the observed values at all times. The model-measurement difference, Δ, increases throughout the day, i.e., predicted glyoxal is larger by a factor of 2.7 (Δ = 370 pptv) at 9:30 am, 3.3 (Δ = 800 pptv) at 11 am, and 3.8 (Δ = 1800 pptv) at 3 pm. This latter difference is more than ten times the 2σ uncertainty of the measurements, and more than three times the 2σ combined model-measurement uncertainty. Figure 1a demonstrates that significantly more glyoxal is produced than observed; an additional glyoxal sink is needed in order to explain gas-phase glyoxal observations.

4. Uptake of Glyoxal Onto Aerosols

[10] Figure 1b demonstrates that the missing sink can be fully accounted with a single parameterization by uptake into the aerosol, either as irreversible glyoxal loss to *S* (MCM_{γ}), or as reversible glyoxal partitioning to *ALW* (MCM_{Heff}) or *OOA* (MCM_{Peff}). MCM_{γ} predicts the measured gas-phase glyoxal throughout the day within the uncertainties with $\gamma = 0.0037^{+0.0028}_{-0.0013}$; MCM_{Heff} with $\rho = 8^{+2.4}_{-2.0} \times 10^8$; MCM_{Peff} with $\zeta = 6^{+1.2}_{-2.2} \times 10^{-9}$; error bars reflect 2σ uncertainty of the combined model + measurement error. In order to match glyoxal observations in the mid morning, slightly larger sinks are needed (Table 1). The "missing" gas-phase glyoxal corresponds to several μg m^{-3} of equivalent SOA mass (Figure 1c). The equivalent SOA mass is comparable to all SOA produced from traditional SOA precursor VOCs. While the results from glyoxal may not easily be transferable to other simple carbonyls [*Kroll et al.*, 2005], species with a similar functionality to glyoxal may in principle add further SOA. The timing of the glyoxal imbalance is fully compatible with the timing of the unaccounted SOA source during that same case study. The glyoxal imbalance can explain 15 to 25% of the observed *OOA* mass [*Volkamer et al.*, 2006]. Ongoing updates to the OH calibration (William H. Brune, personal communication) will increase measured OH, and thus the

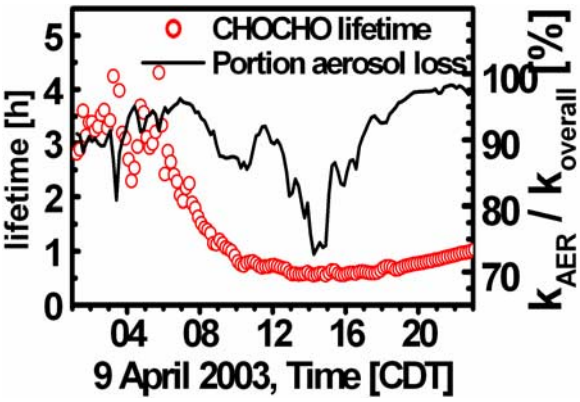

Figure 2. Potential effect of aerosols on the atmospheric lifetime of CHOCHO. An upper limit for the portion of aerosol related losses is calculated from MCM_{γ} (right scale); for MCM_{Heff} and MCM_{Peff} aerosol loss does not affect the atmospheric lifetime.

portion of glyoxal related SOA estimated here is a lower limit; the portion could be as high as 30% at 3 pm.

[11] Sensitivity tests with the dilution rate multiplied by five (dilution case II in [*Volkamer et al.*, 2007]) reduce glyoxal concentrations by about 30% at 3 pm; still three times more glyoxal is predicted than measured. This weak sensitivity to dilution losses is due to the short atmospheric lifetime of glyoxal, which is capped by rapid reactions with OH-radicals and photolysis, limiting the distance over which glyoxal can be transported during the day. Further, dry-deposition losses are bound as an estimated upper limit due to the low PBL [see *Volkamer et al.*, 2006, Figure 1a]. In addition, glyoxal and aromatic precursor VOCs were measured over similar spatial scales using LP-DOAS, making spatial concentration gradients an unlikely explanation for the differences. Since glyoxal forms primarily from an airborne source, a more homogeneous distribution is expected than that of its VOC precursors, for which spatial gradients are small (<15% for most aromatics and CO, <50% for toluene) [*Dunlea et al.*, 2006; T. Jobson et al., submitted manuscript, 2007].

[12] Interestingly, the effective γ values in Table 1 are bracketed by those measured in the laboratory for aqueous inorganic aerosols (0.0008 to 0.0066) [*Liggio et al.*, 2005a] and on cloud droplets/ice crystals ($\leq$0.001 to 0.009) [*Schweitzer et al.*, 1998]. However, *Liggio et al.* observed $\gamma > 0.0023$ only for more acidic particles than those reported here. Similarly, *Schweitzer et al.* observed $\gamma > 0.001$ only for much lower temperatures. The apparent agreement between γ values thus seems to be coincidental. Moreover, the tendency for decreasing γ-values (Table 1) while particle *pH* remains constant (Figure 1) is inconsistent with observations of acid-controlled uptake by *Liggio et al.* Our results do not rule out the possibility of an acid effect, but it is noted that mildly acidic particles (*pH* = 4) may behave differently than the neutral or very acidic particles studied to date. Further, *Kroll et al.* [2005] reproduced experiments by *Liggio et al.* extending experiment times, and did not find any enhanced glyoxal uptake upon acidifying metastable (aqueous) ammonium sulfate particles with sulfuric acid. Rather, they observed that initial glyoxal uptake slowed and reached a plateau after several hours. They concluded that glyoxal uptake is reversible. An increasing uptake over several hours is inconsistent with the tendency for a decreasing time trend in our sink parameterizations (Table 1). *Kroll et al.* also speculated that a "salting-in" mechanism may be controlled by the high *IS* of the particles. Such a mechanism is not compatible with our data; if anything, a slightly smaller sink is observed as *IS* more than doubles in the later day. Finally, activity coefficient models predict typical ζ-values to range from 0.7 to 500 [*Bowman and Melton*, 2004]; the ζ-values in Table 1 can not be explained by physical partitioning into SOA. However, it is well known that rapid chemical reactions occur if glyoxal is in contact with liquid water or dissolved inorganics, i.e., sulfate. In the condensed aqueous phase the currently identified reaction products include mono- and di-hydrates of glyoxal mono-, di-, and trimers (oligomers) [*Whipple*, 1970; *Kielhorn et al.*, 2004], and organo-sulfates [*Liggio et al.*, 2005b]. These products have oxygen-to-carbon ratios in excess of one; further they increase the effective glyoxal solubility. The $H_{eff} = 2.6 \times 10^7$ M atm^{-1} (or $\rho = 5.4 \times 10^6$) observed by *Kroll et al.* [2005] corresponds to several 10 ng m^{-3} of equivalent SOA mass in our case-study. This is about a factor of 150 too small to explain the glyoxal imbalance. The factors that control the additional glyoxal sink remain to be determined. According to Table 1, acetylene, the lightest VOC after methane, should form SOA. Preliminary laboratory experiments have confirmed this, and show significantly higher uptake on mixed organic/inorganic aerosols compared to previous studies of inorganic aerosols (R. Volkamer et al., Secondary organic aerosol formation from acetylene: Seed, acid and RH dependence of glyoxal uptake to aerosols, manuscript in preparation, 2007).

[13] As is shown in Figure 2, the missing glyoxal sink has the potential to strongly affect the atmospheric lifetime of gas-phase glyoxal. The irreversible loss rate of MCM_{γ} accounts for 95% of the glyoxal loss rate at night, and remains the predominant loss process at noontime. The corresponding atmospheric lifetime is 30 min (Table 1). These results may explain why despite active VOC oxidation at night the glyoxal concentrations in the MCMA remain close to or below the detection limit. Abundant $PM_{2.5}$ along with differences in VOC precursors and oxidant fields may explain why glyoxal concentrations in the MCMA are up to a factor of two lower than in Hong Kong [*Ho and Yu*, 2002], and other (somewhat less polluted) urban environments, like Central Los Angeles, Azusa and Claremont [*Grosjean et al.*, 1996].

[14] Finally, we consider these results in terms of the current understanding of the SOA formation mechanism. According to the traditional view, SOA forms when semivolatile products of the gas-phase oxidation of VOCs partition by absorption (dissolution) into an organic particle phase [*Odum et al.*, 1997; *Robinson et al.*, 2007]; the vapor pressure of the partitioning products decreases with the number of carbon-atoms of VOC precursors. Glyoxal uptake to particles questions this volatility scale. Our results emphasize the need to better understand chemical reactions in/on particles, e.g., organic phase-, aqueous phase-, and multiphase processing (i.e. surface, bulk). Such alternative SOA formation routes are increasingly being recognized but

not yet represented in most atmospheric models. SOA formation from glyoxal reaction products is likely to increase the oxygen-to-carbon ratio of ambient SOA.

[15] **Acknowledgments.** We thank Ulrich Platt for lending us the DOAS and spectroradiometer equipment, and Kirsten Johnson, Claudia Hak, Jens Bossmeyer for helping set-up. Coworkers at CENICA and staff at Museo Fuego Nuevo provided kind hospitality during the campaign. Financial support from National Science Foundation (NSF ATM-0308748, ATM-0449815, ATM-0513116, ATM-0528634, ATM-0528227), Alliance for Global Sustainability (AGS), Atmospheric Science Program of the US DOE (DE-FG02-05ER63980, DE-FG02-05ER63981), and Comisión Ambiental Metropolitana (CAM) is gratefully acknowledged. R.V. acknowledges consecutive fellowships by the Henry & Camille Dreyfus Foundation and Alexander von Humboldt Foundation.

References

Bloss, C., et al. (2005), Development of a detailed chemical mechanism (MCMv3.1) for the atmospheric oxidation of aromatic hydrocarbons, *Atmos. Chem. Phys.*, *5*, 641–664.

Bowman, F. M., and J. A. Melton (2004), Effect of activity coefficient models on predictions of secondary organic aerosol partitioning, *J. Aerosol Sci.*, *35*, 1415–1438.

Calvert, J. G., et al. (2000), *The Mechanisms of Atmospheric Oxidation of the Alkenes*, Oxford Univ. Press, New York.

Calvert, J. G., et al. (2002), *The Mechanisms of Atmospheric Oxidation of Aromatic Hydrocarbons*, Oxford Univ. Press, New York.

de Foy, B., et al. (2005), Mexico City basin wind circulation during the MCMA-2003 field campaign, *Atmos. Chem. Phys. Discuss.*, *5*, 2503–2558.

Dunlea, E. J., et al. (2006), Technical note: Evaluation of standard ultraviolet absorption ozone monitors in a polluted urban environment, *Atmos. Chem. Phys.*, *6*, 3136–3180.

Feierabend, K. J., R. K. Talukdar, L. Zhu, A. R. Ravishankara, and J. B. Burkholder (2006), Rate coefficients for the OH + (CHO)2(glyoxal) reaction between 240 and 400 K, *Eos Trans. AGU*, *87*(52), Fall Meet. Suppl., Abstract A23A-0926.

Garcia, A. R., et al. (2006), Separation of emitted and photochemical formaldehyde in Mexico City using a statistical analysis and a new pair of gas-phase tracers, *Atmos. Chem. Phys.*, *5*, 4545–4557.

Grosjean, E., et al. (1996), Air quality model evaluation data for organics: 2. C_1–C_{14} carbonyls in Los Angeles air, *Environ. Sci. Technol.*, *30*, 2687–2703.

Ho, S. S. H., and J. Z. Yu (2002), Feasibility of collection and analysis of airborne carbonyls by on-sorbent derivatization and thermal desorption, *Anal. Chem.*, *74*, 1232–1240.

Jang, M. S., et al. (2002), Heterogeneous atmospheric aerosol production by acid-catalyzed particle-phase reactions, *Science*, *298*, 814–817.

Johnson, K. S., et al. (2006), Aerosol composition and source apportionment in the Mexico City Metropolitan Area with PIXE/PESA/STIM and multivariate analysis, *Atmos. Chem. Phys.*, *6*, 4591–4600.

Kroll, J. H., N. L. Ng, S. M. Murphy, V. Varutbangkul, R. C. Flagan, and J. H. Seinfeld (2005), Chamber studies of secondary organic aerosol growth by reactive uptake of simple carbonyl compounds, *J. Geophys. Res.*, *110*, D23207, doi:10.1029/2005JD006004.

Kielhorn, J., et al. (2004), *Glyoxal*, *Concise Intl. Chem. Assess. Doc.*, vol. 57, World Health Organiz., Geneva, Switzerland.

Kurosu, T., K. Chance, and R. Volkamer (2005), Global measurements of OClO, BrO, HCHO, and CHO-CHO from the Ozone Monitoring Instruments on EOS Aura, *Eos Trans. AGU*, *86*(52), Fall Meet. Suppl., Abstract A54B-01.

Liggio, J., S.-M. Li, and R. McLaren (2005a), Reactive uptake of glyoxal by particulate matter, *J. Geophys. Res.*, *110*, D10304, doi:10.1029/2004JD005113.

Liggio, J., et al. (2005b), Heterogeneous reactions of glyoxal on particulate matter: Identification of acetals and sulfate esters, *Environ. Sci. Technol.*, *39*, 1532–1541.

Lim, H. J., et al. (2005), Isoprene forms secondary organic aerosol through cloud processing: Model simulations, *Environ. Sci. Technol.*, *39*, 4441–4446.

Loeffler, K. W., et al. (2006), Oligomer formation in evaporating aqueous glyoxal and methyl glyoxal solutions, *Environ. Sci. Technol.*, *40*, 6318–6323.

Odum, J. R., et al. (1997), The atmospheric aerosol-forming potential of whole gasoline vapor, *Science*, *276*, 96–99.

Pankow, J. F. (1994), An absorption-model of the gas aerosol partitioning involved in the formation of secondary organic aerosol, *Atmos. Environ.*, *28*, 189–193.

Pirjola, L., et al. (1999), Formation of sulphuric acid aerosols and cloud condensation nuclei: An expression for significant nucleation and model comparison, *J. Aerosol Sci.*, *30*, 1079–1094.

Robinson, A. L., et al. (2007), Rethinking organic aerosols: Semivolatile emissions and photochemical aging, *Science*, *315*, 1259–1262.

Salcedo, D., et al. (2006), Characterization of ambient aerosols in Mexico City during the MCMA-2003 campaign with aerosol mass spectrometry: Results at the CENICA supersite, *Atmos. Chem. Phys.*, *6*, 925–946.

San Martini, F., et al. (2006), Implementation of a Markov Chain Monte Carlo method to inorganic aerosol modeling of observations from the MCMA-2003 campaign. Part II: Model application to the CENICA, Pedregal and Santa Ana sites, *Atmos. Chem. Phys.*, *6*, 4889–4904.

Schweitzer, F., et al. (1998), Uptake rate measurements of methanesulfonic acid and glyoxal by aqueous droplets, *J. Phys. Chem. A*, *102*, 593–600.

Shirley, T. R., et al. (2006), Atmospheric oxidation in the Mexico City Metropolitan Area (MCMA) during April 2003, *Atmos. Chem. Phys.*, *6*, 2753–2765.

Sinreich, R., et al. (2007), MAX-DOAS detection of glyoxal during ICARTT 2004, *Atmos. Chem. Phys.*, *7*, 1293–1303.

Tadic, J., et al. (2006), Photolysis of glyoxal in air, *J. Photochem. Photobiol. A*, *177*, 116–124.

Velasco, E., et al. (2007), Distribution, magnitudes, reactivities, ratios and diurnal patterns of volatile organic compounds in the Valley of Mexico during the MCMA 2002 and 2003 field campaigns, *Atmos. Chem. Phys.*, *7*, 329–353.

Volkamer, R., et al. (2001), Primary and secondary glyoxal formation from aromatics: Experimental evidence for the bicycloalkyl-radical pathway from benzene, toluene, and p-xylene, *J. Phys. Chem. A*, *105*, 7865–7874.

Volkamer, R., L. T. Molina, M. J. Molina, T. Shirley, and W. H. Brune (2005a), DOAS measurement of glyoxal as an indicator for fast VOC chemistry in urban air, *Geophys. Res. Lett.*, *32*, L08806, doi:10.1029/2005GL022616.

Volkamer, R., et al. (2005b), High-resolution absorption cross-section of Glyoxal in the UV/vis and IR spectral ranges, *J. Photochem. Photobiol. A*, *172*, 35–46.

Volkamer, R., et al. (2005c), Remote sensing of glyoxal by Differential Optical Absorption Spectroscopy (DOAS): Advancements in simulation chamber and field experiments, in *Environmental Simulation Chambers: Application to Atmospheric Chemical Processes*, edited by K. Rudzinski and I. Barnes, *NATO Sci. Ser.*, *IV Earth Environ. Sci.*, vol. 62, pp. 129–142, Kluwer Acad., Dordrecht, Netherlands.

Volkamer, R., J. L. Jimenez, F. San Martini, K. Dzepina, Q. Zhang, D. Salcedo, L. T. Molina, D. R. Worsnop, and M. J. Molina (2006), Secondary organic aerosol formation from anthropogenic air pollution: Rapid and higher than expected, *Geophys. Res. Lett.*, *33*, L17811, doi:10.1029/2006GL026899.

Volkamer, R., et al. (2007), Oxidative capacity of the Mexico City atmosphere. Part 1: A radical source perspective, *Atmos. Chem. Phys. Disc.*, *7*, 5365–5412.

Whipple, E. B. (1970), The structure of glyoxal in water, *J. Am. Chem. Soc.*, *92*(24), 7183–7186.

Wittrock, F., A. Richter, H. Oetjen, J. P. Burrows, M. Kanakidou, S. Myriokefalitakis, R. Volkamer, S. Beirle, U. Platt, and T. Wagner (2006), Simultaneous global observations of glyoxal and formaldehyde from space, *Geophys. Res. Lett.*, *33*, L16804, doi:10.1029/2006GL026310.

J. L. Jimenez and R. Volkamer, Department of Chemistry and Biochemistry and CIRES, University of Colorado, UCB 215, Boulder, CO 80309-0215, USA. (rainer.volkamer@colorado.edu)

L. T. Molina, MCE2, 3262 Holiday Court, Suite 201, La Jolla CA, 92037, USA.

M. J. Molina, Department of Chemistry and Biochemistry, University of California, San Diego, Urey Hall 3104, 9500 Gilman Drive, MC 0356, La Jolla, CA 92093-0356, USA.

D. Salcedo, Centro de Investigaciones Químicas, Universidad Autónoma del Estado de Morelos, Avenida Universidad 1001, Cuernavaca, MOR 62209, México.

F. San Martini, Board on Chemical Sciences and Technology, National Academies, 500 5th Street, NW, Washington, DC 20001, USA.